THE JOURNAL OF PHYSICAL CHEMISTRY C

Article

pubs.acs.org/JPCC

New Class of Molecular Conductance Switches Based on the [1,3]-Silyl Migration from Silanes to Silenes

Henrik Löfås,[†] Andreas Orthaber,[‡] Burkhard O. Jahn,[§] Alvi M. Rouf,[§,∥] Anton Grigoriev,*[,†] Sascha Ott,[‡] Rajeev Ahuja,[†,⊥] and Henrik Ottosson*[,§]

[†]Department of Physics and Astronomy, Uppsala University, Box 516, SE-75120, Uppsala, Sweden

[‡]Department of Chemistry - Ångström, Uppsala University, Box 523, SE-75120, Uppsala, Sweden

[§]Department of Chemistry - BMC, Uppsala University, Box 576, SE-75123, Uppsala, Sweden

[∥]Institute of Chemistry, University of the Punjab, New Campus, P.O. Box 54590, Lahore, Pakistan

[⊥]Materials Physics, Department of Materials and Engineering, Royal Institute of Technology (KTH), SE-10044, Stockholm, Sweden

Supporting Information

ABSTRACT: On the basis of first-principles density functional theory calculations, we propose a new molecular photoswitch which exploits a photochemical [1,3]-silyl(germyl) shift leading from a silane to a silene (a Si═C double bonded compound). The silanes investigated herein act as the OFF state, with tetrahedral saturated silicon atoms disrupting the conjugation through the molecules. The silenes, on the other hand, have conjugated paths spanning over the complete molecules and thus act as the ON state. We calculate ON/OFF conductance ratios in the range of 10−50 at a voltage of +1 V. In the low bias regime, the ON/OFF ratio increases to a range of 200−1150. The reverse reaction could be triggered thermally or photolytically, with the silene being slightly higher in relative energy than the silane. The calculated activation barriers for the thermal back-rearrangement of the migrating group can be tuned and are in the range 108−171 kJ/mol for the switches examined herein. The first-principles calculations together with a simple one-level model show that the high ON/OFF ratio in the molecule assembled in a solid state device is due to changes in the energy position of the frontier molecular orbitals compared to the Fermi energy of the electrodes, in combination with an increased effective coupling between the molecule and the electrodes for the ON state.

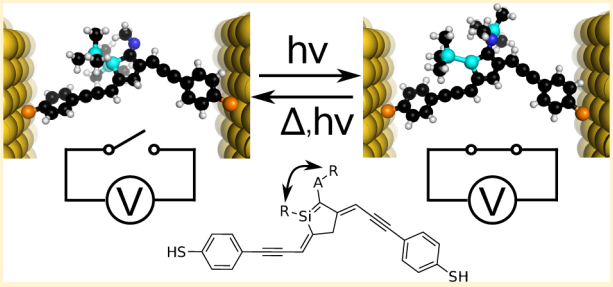

INTRODUCTION

A single molecule that functions as a molecular conductance switch under external stimuli can be useful for molecular memory and logic devices.[1,2] A broad range of molecular switches have been reported in the literature,[2−4] activated with different kinds of external stimuli. Light is a very attractive stimulus due to its fast response time and compatibility with already existing experimental setups.[4] The existing switches can roughly be divided into two categories: redox/polarization switches,[5−7] where the molecule (or part of it) takes up or loses an electron, or isomerization switches,[8−15] where the 3D-structure (geometry and/or connectivity) of the molecule is changed. The basic requirements for a molecular reaction to be suitable for switching applications are: (i) it must have high difference in the magnitude of the conductance for the ON and OFF states, i.e., high switching ratio (SR), (ii) it must be stable, and (iii) it needs a sufficiently high barrier between the ON and the OFF states to hinder accidental (de)activation.[4]

Isomerization switches should ideally have the ON state represented by a planar compound with a linearly conjugated path with maximal pπ-orbital overlap. The compound representing the OFF state, on the other hand, should have a disruption in its pπ-conjugation, and such a disruption could be accomplished by a saturated molecular segment (*structural isomerization*) or by a large twist in the conjugated path (*stereoisomerization*). At the same time, for a possible use in a solid state device the length of the molecule should stay essentially the same which has been a major drawback for some of the previously studied molecular photoswitches, i.e., azobenzenes.[11−13] Further, it should be possible to switch the molecule between the two states with an external stimulus, and most interesting is the possibility to switch in one direction with one stimulus and in the other direction with another stimulus.

The [1,3]-silyl shift for formation of a Si═C double bonded compound, a so-called silene,[19−23] from an acyloligosilane is a structural isomerization that potentially could be used for a novel type of molecular switch. This reaction was used by Brook and co-workers to form the first isolable silene in 1981 (Scheme 1).[16,17] Importantly, the acyloligosilanes such as **1a**-

Received: January 3, 2013
Revised: April 2, 2013
Published: April 5, 2013

   dx.doi.org/10.1021/jp400062y | J. Phys. Chem. C 2013, 117, 10909−10918

OFF and **1b-OFF** were turned into the Brook-silenes photolytically through irradiation by mercury spot lamps. However, it was also observed that the silenes rearranged back to the acyloligosilanes (e.g., silene **1b-ON** has a half-life of 15.8 h at 25 °C in ether solution).[16] Silene **1a-ON**, on the other hand, could be observed spectroscopically (IR, UV, NMR) over a period of two weeks at room temperature, during which it gradually rearranged back to **1a-OFF**. With regard to **1a-OFF**/**1a-ON**, we report herein (vide infra) the calculated reaction energy for **1a-ON** formation to be 51.2 kJ/mol, and the activation energy for the thermal back-rearrangement from the silene to silane to be 82.1 kJ/mol (Scheme 1). In a recent computational study, Eklöf, Guliashvili, and Ottosson found silene **1c-ON** to be 20.1 kJ/mol higher in energy then **1c-OFF**, and an activation barrier of 123.4 kJ/mol separated the silene from the acyloligosilane.[18] This property of the acyloligosilane/Brook-silene system should be possible to elaborate further and potentially exploit in a molecular conductance switch. The described activation energies for thermal back-rearrangements from the silene to the silane to progress at moderately elevated temperatures should be in the range 90−120 kJ/mol, and the reaction energies for this process should be moderately exothermic.

Scheme 1. Photochemical [1,3]-Silyl Shift of Acyloligosilanes 1-OFF to Their Isomeric Brook-Silenes 1-ON and the Thermal Back-Rearrangement (1a R = *t*-Bu, 1b R = Adamantyl,[16,17] and 1c R = Me[18])[a]

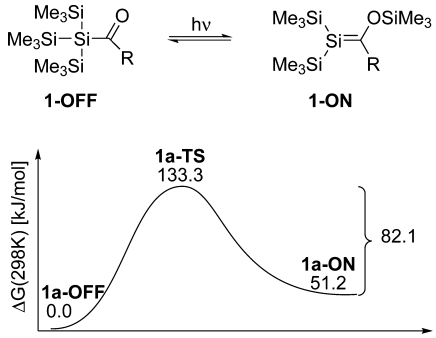

[a]Reaction and activation free energies for the thermal processes of **1a** computed at the B3LYP/6-31G(d) level as reported herein (vide infra). Transition state abbreviated as TS.

Our earlier computational study showed a distinct difference in the relative energies between the Brook-type 1,1-dimethylsilenes as compared to the analogous Brook-type 1,1-bis(trimethylsilyl)silenes where the former have higher relative energies by 40−60 kJ/mol compared to the latter species.[18] This feature is interesting as an acyloligosilane/Brook-silene switch should have the silene (the ON state) slightly higher in energy than the acyloligosilane (the OFF state) so that a driving force for the thermal back-rearrangement is established. Consequently, the relative energy of silene versus acyloligosilane can be tuned by a proper choice of substituents at the central Si. Moreover, a change from a migrating silyl group to a migrating germyl (stannyl) group weakens the O−E bond strength (E_{O-E} = Si > Ge > Sn), raising the energy of the silene (ON) side. Increased steric bulk of the migrating group should also disfavor the acylsilane (OFF) side as recently found by Bravo-Zhivotovskii et al.[24] Finally, one can expect that increased conjugation, as found in the silenes studied herein, will lower the relative energies of these species. Our initial model species for the acylsilane/Brook-silene switches, together with their carbon analogues, are displayed in Scheme 2. These model silenes have a linearly conjugated path stretching between the two ends of the molecule, whereas the acyloligosilanes have an interruption. We first examine the acyloligosilane/Brook-silenes in their *trans*-conformers with thiol end groups since those (still) are ubiquitous anchors to gold electrodes, even though a range of other groups with improved anchoring properties recently have been identified.[25,26]

Scheme 2. Potential Acyloligosilane/Brook-Silene Switches and Their Carbon Analogues, Where R = −CC−C_6H_4− for a and R = −C_6H_4− for b

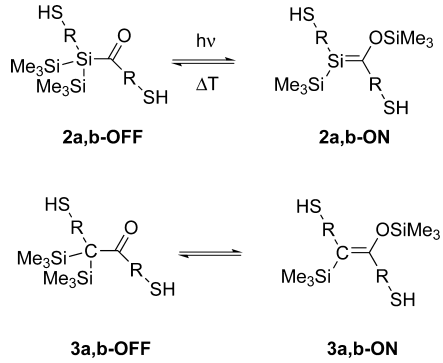

Thus, we report on a new class of constitutional molecular switches based on the [1,3]-silyl shift going from a silane to a silene. We start by the linear acyloligosilane/Brook-silene molecules where we calculate the reaction (rxn) and activation energies as well as the transport properties using density functional theory (DFT) and nonequilibrium Green's functions (NEGF). However, based on our work on these linear switches, we found that it is important to constrain the motion when the system progresses along the reaction coordinate over the transition state (TS). Consequently, these first candidates needed to be further modified to perform optimally as molecular conductance switches in solid state devices. The second half of the study is therefore devoted to computational design of a set of more realistic molecular switch candidates. Reaction and activation energies were computed for the new cyclic silane/silene switches, where we also find constrained motions. Furthermore, transport investigations reveal high switching ratios. Using a single-level transport model, we estimate the location of the most dominating level for electron transport (E_0) and the broadening of the level (Γ) and their influence on the switching ratio.

COMPUTATIONAL METHODS

Full geometry optimizations without symmetry constraints were carried out with the Gaussian09 program package.[27] All geometry optimizations reported were performed with the B3LYP hybrid density functional theory (DFT) method in combination with the 6-31G(d) valence double-ζ basis set.[28−30] Frequencies were computed to confirm that the calculated structures correspond to local minima or transition states on the potential energy surface.

The B3LYP hybrid DFT method was chosen as we earlier have found that the deviations in the geometries of a set of 15 small substituted silenes in a total of 27 different conformers,

dx.doi.org/10.1021/jp400062y | J. Phys. Chem. C 2013, 117, 10909−10918

Table 1. Free Energies for Silyl Shifts from OFF to ON States (Schemes 1 and 2)

compound	ΔG_{rxn} [b]	$\Delta G^{\ddagger}_{OFF \rightarrow ON\ (ON \rightarrow OFF)}$ [c,d]	S···S distance[a] ON	OFF	TS
1a	51.2	133.3 (*82.1*)	-	-	-
2a	−20.5	125.4 (*145.9*)	18.63	18.50	11.72
2b	1.0	116.8 (*115.7*)	13.57	13.54	9.51
2b* [e]	1.0	191.1[e] (*190.0*)[e]	13.57	13.54	13.54[e]
3a	−105.0	-	18.09	17.99	-
3b	−140.7	-	12.99	12.35	-

[a]Distance between thiol end groups [Å]. [b]Reaction free energy [kJ/mol]. [c]Free energy of activation relative to the OFF-state (normal print) [kJ/mol]. [d]Free energy of activation relative to the ON-state (*in italics*) [kJ/mol]. [e]Restricted S···S distance.

including silenes with natural ($Si^{\delta+}$=$C^{\delta-}$) as well as reverse ($Si^{\delta-}$=$C^{\delta+}$) bond polarization, when compared against CCSD/cc-pVTZ geometries, are smallest for hybrid DFT methods.[31] Neither MP2 nor generalized gradient approximation (GGA) DFT methods, as computationally inexpensive methods, lead to better agreements. The M06-2X meta-hybrid GGA DFT method[32,33] was found to give a slightly better mean absolute deviation but, on the other hand, gave spurious geometry deviations for a few of the test silenes when compared against the CCSD geometries. We therefore based the present study on B3LYP computations. The effect of the basis set on the calculated geometries was also examined on the test set of small silenes mentioned above, and it was revealed that the mean absolute deviation, as compared to CCSD/cc-pVTZ, was 0.017 and 0.019 Å with regard to the Si=C double bond lengths calculated at B3LYP/cc-pVTZ and B3LYP/6-31G(d), respectively. For the **15-OFF/15-ON** and **17-OFF/17-ON** silane/silene switches, we also examined the quality of the B3LYP/6-31G(d) calculations with regard to basis set and with regard to treatment of sterically congested situations (dispersion). B3LYP calculations with the 6-31G(d) valence double-ζ basis set were compared against B3LYP calculations with the 6-311+G(d,p) valence triple-ζ basis set,[34] and both reaction and activation energies when calculated at the B3LYP/6-311+G(d,p)//B3LYP/6-31G(d) level were found to agree well (see Supporting Information). When the B3LYP/6-31G(d) energies are compared against calculations with the M06-2X hybrid meta GGA functional, i.e., a dispersion corrected functional which is better able to describe sterically congested situations, it was also found that the deviations in energies were modest (see Supporting Information).

Time-dependent DFT (TD-DFT) calculation were carried out with B3LYP in combination with a 6-311+G(2d,p) basis set, considering ten transitions each (singlets and triplets).

Transport calculations were carried out from first principles with a method based on nonequilibrium Green's functions (NEGF) combined with DFT as implemented in the TranSIESTA package.[35] The relaxed molecular structures were inserted as their dithiolates between two Au[111] surfaces and relaxed once more to optimize the Au−S bonding. The device consists of three parts: left electrode, molecule, and right electrode. The electrodes are modeled by six layers of gold atoms where the three outer layers are relaxed, while the others are kept at the experimental bulk positions. In the lateral dimension a 6 × 6 supercell (17.5 Å × 17.5 Å) was used, large enough to remove interactions between periodic images. All relaxations are performed at the DFT level with the SIESTA package,[36,37] and core electrons are modeled using Troullier-Martins[38] soft norm-conserving pseudopotentials. The valence electrons are expanded in a basis set of local orbitals using a double-ζ plus polarization orbital (DZP) set for electrons in the molecule and a single-ζ plus polarization orbital (SZP) for electrons in the gold electrode. The GGA was used for the exchange-correlation functional.[39]

RESULTS AND DISCUSSION

Structural Calculations of Isolated Acyloligosilanes and Brook-Silenes. The OFF states of switches **2a**, **2b**, **3a**, and **3b** were optimized in the *anti*-conformers, and the ON states were optimized as *E*-isomers to match the expected structures of a rigidly confined acyloligosilane/Brook-silene switch. For these species, it becomes clear that for the two acyloligosilane/Brook-silene pairs the acyloligosilane and the silene side are nearly isoenergetic (see Table 1), while for the all-carbon α-silyl ketone/siloxyalkene pair the alkene is much lower in energy. The very large difference in relative energy for the two sides of the all-carbon pairs can not be changed significantly through substitution, and our calculations thereby reveal why the [1,3]-silyl shift to form an alkene, and the reverse reaction, are not suitable to function as a reversible molecular switch. The [1,3]-shift of a silyl group from the α-carbon of a ketone to the carbonyl oxygen is thus a purely hypothetical molecular switching reaction. However, with a suitable tailoring of the acyloligosilane/Brook-silene switch pair, it should be possible to design a system with the silene slightly above the acyloligosilane in energy and which has an activation energy for the thermal back-reaction which is reasonably high (90−120 kJ/mol) so that moderately elevated temperatures can be used to turn off the switch. The activation energy for the [1,3]-silyl shift from **1a-OFF** to **1a-ON** is calculated to be 133.3 kJ/mol at the B3LYP/6-31G(d) level, but the activation energy for the back-reaction taken relative to **1a-ON** is only 82.1 kJ/mol. As this silene gradually rearranged back to the silane during a period of two weeks, it is obvious that the barrier for a silane/silene switch needs to be slightly higher.

Importantly, the S···S distances within each of the four pairs stay essentially constant when going from the OFF structure to the ON structure; however, investigations of the transition states revealed that the migration of the silyl group requires a significant rotation around the central Si−C bond. This rotation induces a large motion of the two thiol anchors during the (thermal) rearrangement and consequently a significant shortening of the S···S distance to 9.57 Å for **2b-TS**, i.e., a reduction by approximately 4 Å. Attempts to mimic the rather fixed distance situation, as would be seen in a solid-state setup, by virtually fixing the S···S distance to 13.54 Å resulted in a large increase in the activation energy from 115.7 to 190.0 kJ/mol of **2b-TS**, a prohibitively high activation barrier for thermal back-rearrangement at reasonably elevated temperatures.

dx.doi.org/10.1021/jp400062y | J. Phys. Chem. C 2013, 117, 10909−10918

Brook and co-workers used acyloligosilane **1a-OFF** (Scheme 1) to form silene **1a-ON**, which has UV/vis absorption maxima at 348 nm (ε = 100) and 339 nm (ε = 5200), respectively, showing good agreement with TD-DFT calculated values of 362 nm (oscillator strength f = 0.0118) for **1a-OFF** and 351 nm (f = 0.2165) for **1a-ON**. The presently investigated acyloligosilanes **2a-OFF** and **2b-OFF** have their computed lowest UV/vis absorptions with significant calculated oscillator strengths at 395.7 nm (f = 0.1194) and 381.3 nm (f = 0.0352), respectively (see Supporting Information). From this we can conclude that the present silane/silene pairs could form the basis for a light-driven molecular switch under the condition that the motion along the reaction path is constrained.

Current−Voltage Characteristics of Linear Switches. To estimate the switching properties of the acylsilane to silene transition, we performed first-principles DFT calculations for the acetylenic compounds (**2a**/**3a**) shown in Scheme 2. Compounds (**2b**/**3b**) showed a different behavior in the electrode setup which is briefly discussed in the Supporting Information. The current response for bias voltages of ±0.1, ±0.2, ±0.5, and ±1.0 V are shown in Figure 1. Looking at

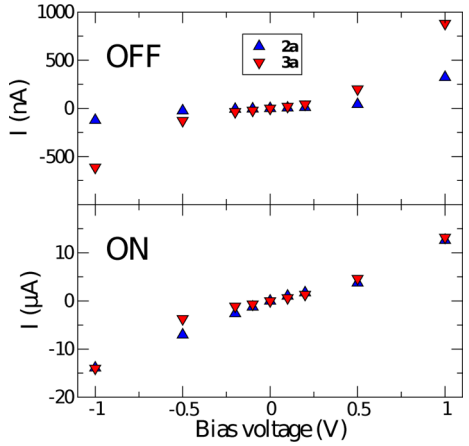

Figure 1. Calculated current−voltage (I−V) characteristics for OFF and ON state structures of compounds **2a** and **3a**, respectively. Note the different scales for the calculated currents in the ON and OFF states.

trends in the current response, both compounds **2**/**3a-OFF** and **2**/**3a-ON** show a similar behavior with a linear increase of the current for low voltages and more rapidly increasing current at higher voltages. To investigate their performance as switches, we calculate the ON/OFF switching ratio of the current for both the zero-bias limit as well as for a bias of +1 V. Due to the unsymmetric nature of these molecules, we also investigate if they have a rectifying property on the current, hence if they could function as diodes.[40] These results are shown in Table 2. The ON/OFF ratio is higher for compound **2a** compared to

Table 2. Current Characteristics of 2a and 3a

compound	SR[a] (0 V)	SR[a] (1 V)	RR[b]
2a-OFF	270	39	2.6
2a-ON			0.9
3a-OFF	31	15	1.4
3a-ON			0.9

[a]Conductance ON/OFF switching ratio. [b]Rectifying ratio, calculated as the ratio between the currents at bias voltages of +1 and −1 V.

the all-carbon switch **3a**. From Figure 1 it can be seen that this is due to a more conducting OFF state for **3a**, while the current response is very similar for the two ON states. When going to higher biases, the switching ratio decreases due to the stronger current response from the low-conducting acyloligosilanes and ketones when the bias is increased.

To explore the physical mechanisms behind the switching, we start by calculating the partial density of states (PDOS) for the junctions with **2a** under equilibrium conditions. The density of states spatial distribution[41] can be calculated by summing up the states in the transverse direction and normalizing to the atomic density. This gives the number of states/(eV × Å × atom) along the transport direction which is shown in Figure 2, where the x-axis is the coordinate along the

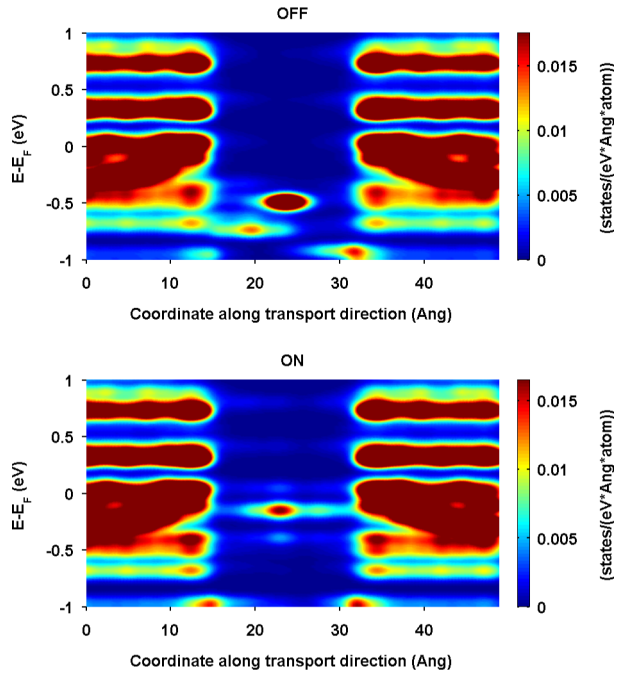

Figure 2. Space resolved normalized density of states at zero bias for the junctions with compound **2a**. The OFF state is shown in the top panel and the ON state in the bottom panel. The space resolved density of states have the transport coordinate on the x-axis and the energy of the state on the y-axis. The color scale goes from blue (low density of states) to red (high density of states).

transport direction and the y-axis shows the energy ($E - E_F$) for the state, where the magnitude of the DOS is indicated by the color, from blue (low) to red (high).

For **2a-OFF** the HOMO of the molecule is located about 0.5 eV below the Fermi level (E_F) of the electrodes and is not so well coupled to the electrodes. The electronic states in the molecule that are induced by the interaction with the metallic electrodes are often referred to as metal-induced gap states (MIGS).[41] MIGS can be seen in the spatial DOS plot as light-blue protrusions penetrating into the molecule from both electrodes but rapidly decaying toward the center of the switch.

The [1,3]-silyl shift leads to the formation of **2a-ON** (**3a-ON**) having a Si═C (C═C) double bond. The DOS spatial distribution for **2a-ON** (bottom panel) shows that the HOMO of the molecule is shifted closer to E_F, and at the same time it is delocalized over the molecule and coupled to both electrodes. MIGS are seen to extend much longer into the molecule. Coupling of the HOMO to the electron states in the electrodes

dx.doi.org/10.1021/jp400062y | J. Phys. Chem. C 2013, 117, 10909−10918

causes broadening of the DOS peak. We see two light blue "satellites" of the HOMO slightly above and below in energy in the DOS spatial distribution plot created by the extended MIGS overlapping with the broad HOMO peak. The broadening and delocalization of the HOMO and surrounding MIGS create a relatively smooth DOS close to the Fermi level. This density is responsible for the absence of current onset around the position of the HOMO (~0.2 or ~0.4 V bias), when increasing the bias voltage for **2a-ON** (**3a-ON**).

Furthermore, we show the wave function of the most conducting scattering state at zero bias in Figure 3.[42] The

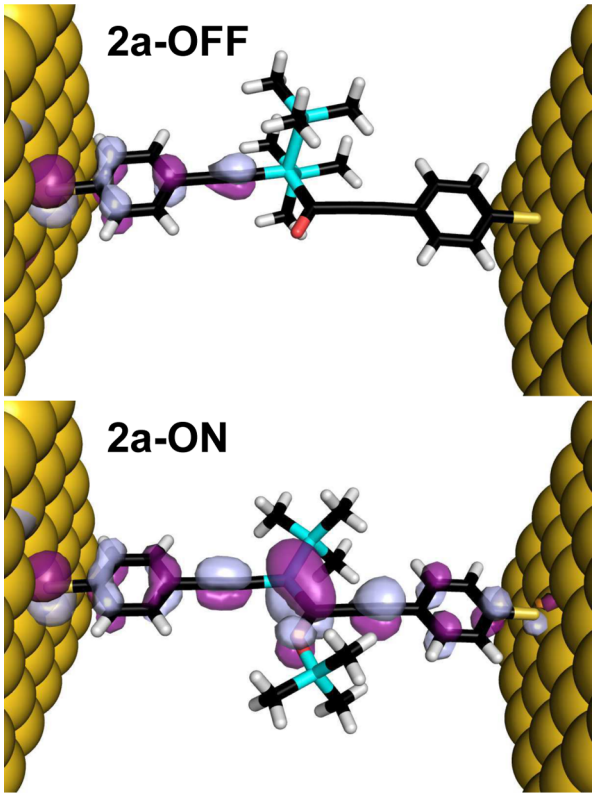

Figure 3. Visualization of the most transmitting eigenchannel wave function (incoming from the left electrode) at the Fermi energy for the junctions with compound **2a**. OFF state shown in the top panel and ON state in the bottom panel. The isosurfaces of the eigenchannel wave function are colored according to phase and sign, the positive/negative real part being colored in deep-purple/light-blue (the imaginary part is below the cutoff value and not visible), and both junctions plotted with the same isovalue to be comparable.

isosurface of the scattering state has different colors depending on the phase (+1, −1, +*i*, −*i*) as explained in the figure caption. The magnitudes of the isosurface lobes indicate where the electrons incoming from the left electrode are traveling since the absolute square of the wave function corresponds to the density of traversing electrons. For a wave, incoming from the left and which is mostly reflected, the real part will show an exponential decay into the junction from the left, while the imaginary part will be very small and in most cases not visible (if the same isovalue is used when plotting). As in the case of DOS spatial distribution for **2a-OFF**, the scattering state (top panel) shows a very weak coupling through the central Si−C bond, where the real part of the state decays rapidly from the left into the junction indicating that in this case we have a poor conductor acting as a tunneling barrier. The imaginary part of the wave function is not visible due to the low transmission of the channel and that the wave function is chosen to be real at the incoming side.

From the scattering state of **2a-ON** (bottom panel) the Si═C double bond formed from the [1,3]-silyl shift shows a good connection through the central bridge providing a higher conductance through the MIGS at the Fermi level. It is still almost only the real part of the wave function that is visible, but it does not decay as fast into the junction. From the shape of the lobes we can see that the main transport goes through the pπ-orbital system of the molecule. Similar conclusions can be drawn for **3a**; i.e., for the ON state we have a very good linear conjugation through the complete molecule, while for the OFF state the conjugation is broken in the central unit due to the Si−C (C−C) single bond; hence, the transmission drops significantly.

Design of Realistic Silane/Silene Switches. Even though the studies of reaction thermodynamics as well as electron transport of **2a**,**b** reveal that these compounds exhibit the desired properties, the large structural change along the reaction pathway led us to a redesign. In particular, the twisting about the central SiC bond that takes place during the [1,3]-silyl shift, leading to drastic variations in the S···S distance during the reaction, needs to be reduced, and a silane/silene unit with less conformational flexibility is required. This can be accomplished by introduction of a fused cyclic system that would prevent large motions leading to/from the TS. However, this restricted system must not have a raised energy of the TS state as this would hamper a thermal back-reaction. To provide a cyclic system with an overall pπ-conjugated pathway in the ON state, we designed a five-membered ring with a central SiC unit having a Si═C double bond and two neighboring exocyclic C═C double bonds. To accommodate for steric congestion, either a benzene or a phenylacetylene group is attached to the double bonds in an all-*trans* arrangement. To provide suitable anchors, we kept the thiol groups in *para*-positions of the phenyl moieties. Our initial studies on the linear silane/silene systems indicate approximately the desired thermodynamic and kinetic properties for a light-triggered ON switch with a back-reaction which is thermally feasible. One advantage of this rearrangement is the possibility of tuning both thermodynamics and kinetics by slight variations. For our further investigations on the cyclic systems, we focused on three parameters: the nature of the migrating group (silyl or germyl), the steric bulk of the migrating group (EMe_3 or E^tBu_2Me, where E = Si or Ge), and the acceptor group (A = O or = NMe) (Figure 4).

Simple variation of these three parameters gives a tremendous impact on the reaction thermodynamics (Table 3). While the silyl migrating groups in combination with an oxygen acceptor favor the ON state (from 1.1 to 52.5 kJ/mol), migration to the nitrogen-based acceptor (an imine in the OFF state) is strongly dependent on the steric bulk of the silyl group (Figure 5). There are further general trends in our calculations. Changing the central atom of the migrating group from silicon to germanium favors the OFF state by up to 76 kJ/mol, depending on the steric demand of the alkyl substituents and the acceptor group. However, a general trend for the two different acceptor groups was not found. We further investigated the transition states for the thermal rearrangement of the cyclic silane/silene combinations with the most promising thermodynamic properties. Introduction of the five-membered ring results in a reduced TS motion and,

dx.doi.org/10.1021/jp400062y | *J. Phys. Chem. C* 2013, 117, 10909−10918

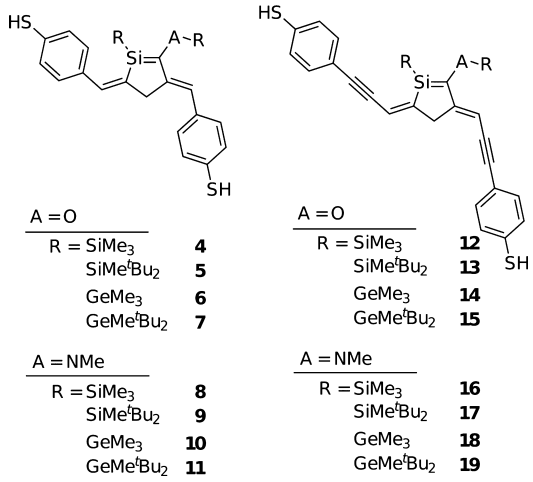

Figure 4. Suggested cyclic molecular conductance switches with different acceptor moieties and migrating groups. A = NMe or O, and R = $SiMe_3$, Si^tBu_2Me, $GeMe_3$, or Ge^tBu_2Me.

Table 3. Free Energy for Silyl Shifts from OFF to ON States for Cyclic Compounds (Figure 4)

			S···S distance[a]		
compound	ΔG_{rxn}[b]	$\Delta G^{\ddagger}_{OFF \rightarrow ON\ (ON \rightarrow OFF)}$[c,d]	ON	OFF	TS
4	−1.1	159.0 (*160.0*)	15.2	15.1	15.3
5	−52.5	-	15.1	15.2	-
6	64.9	-	15.4	15.2	-
7	40.8	-	15.1	15.2	-
8	24.8	132.7 (*107.8*)	15.2	13.7	14.8
9	−0.4	126.9 (*128.4*)	14.5	14.3	15.2
10	63.8	-	14.9	14.4	-
11	76.0	-	14.7	14.5	-
12	−6.8	164.4 (*171.1*)	18.8	19.2	19.4
13	−42.5	-	18.6	18.6	-
14	59.4	-	19.2	19.3	-
15	33.2	158.6 (*125.4*)	18.3	18.5	19.5
16	11.7	139.7 (*128.1*)	18.6	17.9	19.0
17	15.7	159.8 (*144.2*)	17.0	17.8	19.0
18	49.0	-	18.5	18.1	-
19	61.0	-	17.4	17.9	-

[a]Distance between thiol end groups [Å]. [b]Reaction free energy [kJ/mol]. [c]Free energy of activation relative to the OFF state (normal print) [kJ/mol]. [d]Free energy of activation relative to the ON state (*in italics*) [kJ/mol].

moreover, provides suitable kinetic parameters. The activation energies relative to the OFF states are 126−160 kJ/mol. The ON states are in most cases higher in relative energy, which will allow for a thermal back-rearrangement at (slightly) elevated temperatures as the activation free energies for all except one system are gathered in the range 108−144 kJ/mol. The drawbacks of the linear systems, i.e., the large motion leading to/from the TS, were also successfully circumvented by the cyclic silane/silene switches. The largest absolute displacements were calculated to be in the range 0.2−2.0 Å, which corresponds to relative motions of less than 10% of the absolute S···S distance. We assume that these small changes can easily be balanced by lateral movement on the gold substrates, without significant changes in reaction energies.

To prove the viability of photochemically induced silene formation we also performed TD-DFT calculations for the

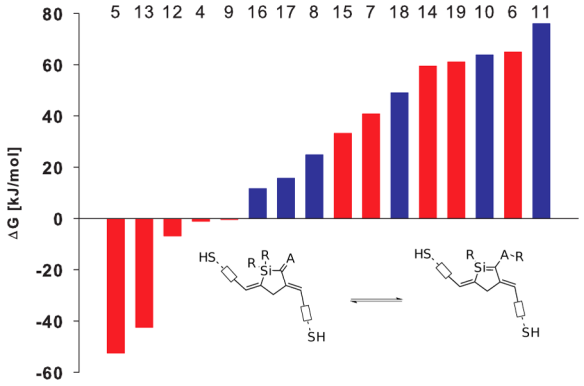

Figure 5. Relative reaction energies for the extended cyclic silane/silene switches. Blue bars denote N acceptor groups (A = NMe), while red bars denote the oxygen acceptors (A = O).

extended cyclic systems **16** and **17** in their ON and OFF configurations. For compound **16-OFF**, the first allowed UV/vis transition should occur at around 416 nm (f = 0.0424) with a stronger absorption at 404 nm (f = 0.2193). Similarly, but slightly red-shifted, we found for **17-OFF** a weaker (417 nm, f = 0.0342) and a stronger (407 nm, f = 0.1301) transition. The extension of the pπ-system in the corresponding silenes, **16-ON** and **17-ON**, is also clearly reflected in the calculated UV/vis spectra of compounds **16-ON** (556 nm, f = 1.1302) and **17-ON** (544 nm, f = 0.9959) as shown by their longest wavelength absorptions. These long-wavelength absorptions for the ON states potentially allow the suggested switches to operate in a reversed manner, in which the ON states might rearrange to the corresponding silanes by irradiation with visible light. However, **16-ON** and **17-ON** also absorb at the shorter wavelengths, and this feature may potentially complicate the formation of the silenes, which when formed can absorb the irradiation used for their generation and photorearrange back to the silanes. Yet, detailed computational and experimental studies and optimization of the photochemistry of the cyclic silane/silene switches are outside the scope of the present investigation. For example, for an optimal silane/silene switch the position of the photostationary state needs to be optimized so that predominantly the silene is formed upon irradiation at the chosen wavelength.

Current−Voltage Characteristics of Cyclic Switches. The current−voltage characteristics have been examined by DFT-NEGF calculations, and due to computational cost we have chosen to study the compounds **4**, **12** (O-acceptor and trimethylsilyl migrating group), **8**, **16** (NMe-acceptor and trimethylsilyl migrating group), and **17** (NMe-acceptor and $SiMe^tBu_2$ migrating group) here. The current−voltage results and their switching ratios are shown in Figure 6 and Table 4, respectively. Compared to the previous linear compound, we find larger switching ratios at zero bias. By introducing the cyclic unit interference effects, similar to those observed by Solomon et al. in phenyl rings,[43] appear in the OFF compounds lowering their transmission close to E_F. This partly explains the higher switching ratios at low bias. The interference effects can clearly be seen in the transmission spectra where there are several pronounced dips for the OFF compounds with the phenylacetylene group (−CC−Ph) shown in the top panel of Figure 7. For the shorter compounds (**4**, **8**) transmission in the σ-system of the molecules can now start to play an important role, and this can hide interference effects in the pπ-system. In

dx.doi.org/10.1021/jp400062y | J. Phys. Chem. C 2013, 117, 10909−10918

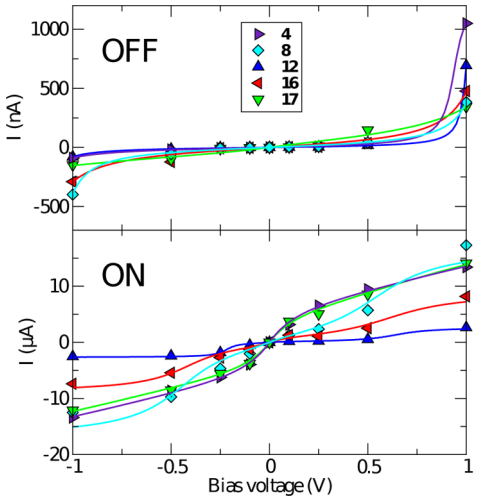

Figure 6. Current−voltage of cyclic switches and model calculations. Markers denote values obtained from the DFT-NEGF calculations, while the full lines are obtained from the model calculations. Note the different scales for the calculated currents in the ON and OFF states.

the top (bottom) panels of Figure 8 the local currents[42,44] in compound **16** are shown for the OFF (ON) state. For the OFF state we find that the interference arises due to ring currents in the ring segment with three saturated carbon atoms. On the other hand, for the ON state we observe an undisturbed current path which follows the pπ-conjugated path through the molecule.

At higher bias, the switching ratio drops to moderate levels for the cyclic compounds similar to the linear analogues. As in the case of the reaction energies we see that the NMe acceptor groups (compounds **8**, **16**, **17**) are the most promising candidates with switching ratios on par or higher compared to other compounds studied here and in previous investigations.[2,10,14,45] Introduction of the bulkier migration group ($SiMe^tBu_2$, compound **17**) not only will provide higher steric protection and hence higher kinetic stability but also enhances the switching ratio. The ON compounds have rectification ratios (RR) close to unity, which is beneficial for practical applications since there will be no directional dependence when running a current through the switch. On the other hand, some of the OFF compounds have large RR (especially compounds

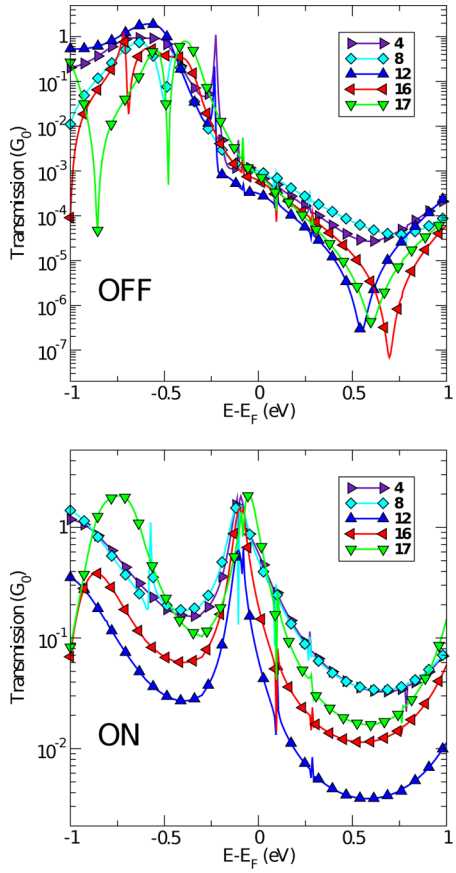

Figure 7. Transmission spectra, at zero bias (V = 0), for the OFF compounds (top panel) and the ON compounds (bottom panel).

with O-acceptor, **4** and **12** in Table 4), opening the possibility to use them as diodes. For switch applications, the RR of the OFF compound is not important since there should be no (or only a negligible) current running through them, but it will give a difference in SR between +1 V and −1 V (here, for RR > 1, the SR at −1 V will be larger than the SR at 1 V).

Similar to Kim et al.[10,14] we apply a simple single-level transport model to investigate the influence of the effective coupling (Γ_L,Γ_R) to the left and the right electrode, and the distance between the closest molecular orbital (E_0) and E_F of

Table 4. Current−Voltage Characteristics of Cyclic Compounds

	DFT-NEGF calculations			model calculations			
compound	SR[a] (0 V)	SR[a] (1 V)	RR[b]	E_0[c] (eV)	Γ[d] (meV) (= $(\Gamma_R\Gamma_L)^{1/2}$)	ε_- (ε_+)[e]	Γ_R/Γ_L[f]
4-OFF	718	13	11.8	0.46	5.5	7.5 (104.3)	13.9
4-ON			1.0	0.08	55.0	2.4 (2.4)	1.0
8-OFF	503	45	1.0	0.50	7.7	24.5 (24.5)	1.0
8-ON			1.4	0.16	36.9	7.2 (5.0)	0.7
12-OFF	203	4	8.7	0.49	4.3	12.8 (74.2)	5.8
12-ON			1.1	0.06	5.7	4.3 (2.5)	0.6
16-OFF	314	17	1.6	0.54	10.1	16.7 (43.4)	2.6
16-ON			1.1	0.09	18.7	3.4 (2.8)	0.8
17-OFF	1157	41	2.3	0.52	13.9	3.6 (7.6)	2.1
17-ON			1.2	0.08	50.0	2.5 (2.6)	1.1

[a]Conductance ON/OFF switching ratio. [b]Rectifying ratio, calculated as the ratio between the current at bias voltage +1 and −1 V. [c]Distance between the most conducting level and E_F (V = 0). [d]Effective coupling between the most conducting level and the electrodes. [e]Proportionally factor for movement of the conducting level under bias ($\tilde{E}_0 = E_0 \pm (V/\varepsilon_\pm)$ for $\pm V$, $\varepsilon_+ = \varepsilon_-\Gamma_R/\Gamma_L$). [f]A measure of the unsymmetry of the effective coupling to the electrodes.

dx.doi.org/10.1021/jp400062y | J. Phys. Chem. C 2013, 117, 10909−10918

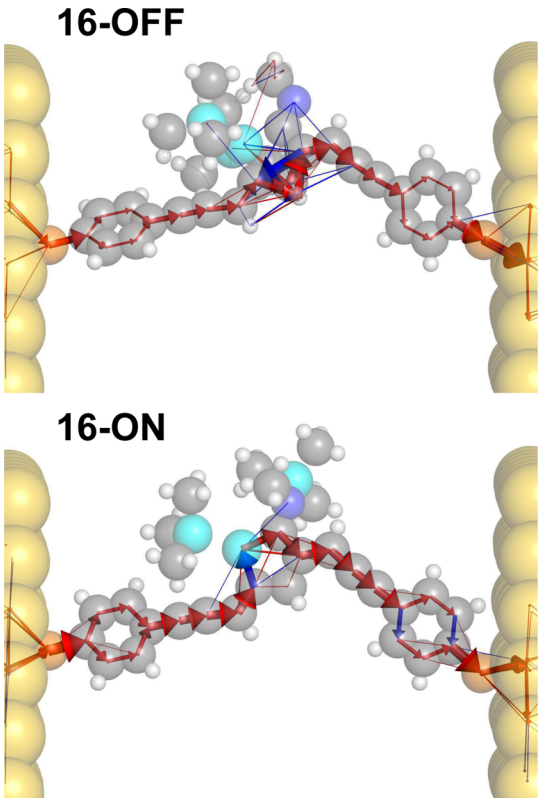

Figure 8. Local currents in compound **16-OFF** (top panel) and **16-ON** (bottom panel), where the cross-sectional area of the cylinder is proportional to the current density. Red currents represent positive transport direction, and blue currents represent negative direction. The currents are calculated at the Fermi energy ($(\mu_L + \mu_R)/2$), but a small positive bias voltage is assumed for calculation purposes. For a full derivation see Okabayashi et al.[44] and Paulsson and Brandbyge.[42]

the electrodes on the current. From the Landauer formula[46,47] the transmission is obtained as

$$T(E) = \frac{4\Gamma_L\Gamma_R}{(E - E_0)^2 + (\Gamma_L + \Gamma_R)^2} \quad (1)$$

We started by considering a static level and symmetric coupling to the electrodes as the earlier literature suggested.[10] Results from this model could not explain our findings. To describe our systems, we had to expand the model with a level that could move with the potential level in the electrodes under bias ($\tilde{E}_0 = E_0 \pm (V/\varepsilon_\pm)$ for $\pm V$, see Table 4 for values of ε) and nonsymmetric coupling to the electrodes. The parameters obtained from the model are given in Table 4, showing that the unsymmetry of the coupling (Γ_L/Γ_R) we find from our model agree reasonable well with the RR of the molecules. The results from the model are shown in Figure 6 (full lines), together with the DFT-NEGF results (markers). As can be seen from the figure, this extended model can explain our results reasonably well. From this model we can locate the most conducting MO at about 0.5 eV below E_F for the OFF states and almost resonant (0.05−0.15 eV below E_F) for the ON states. This can be compared with the transmission spectra at zero bias (shown in Figure 7) from the DFT-NEGF calculations, and we find that the peaks in the spectra are located at similar values as obtained from the model (a comparison between transmission spectra at different biases from DFT-NEGF and our model is shown in the Supporting Information). From the model results we are able to deduce the important parameters affecting the SR. In Figure 9 the magnitude of the SR (symbolized by the size of the filled circles) is shown as a function of the change in coupling to the electrodes ($\Gamma = (\Gamma_L\Gamma_R)^{1/2}$) and the change in distance between the closest MO and E_F. The switching occurs due to either a change of the distance between the closest MO and E_F, a change in the coupling between the MO and the electrodes, or a combination of both. To have a large SR ideally the molecule should be in the top right corner of Figure 9, hence it is favorable to have both a large change in distance between E_F and the closest MO and a large change in the coupling between the electrodes and the MO.

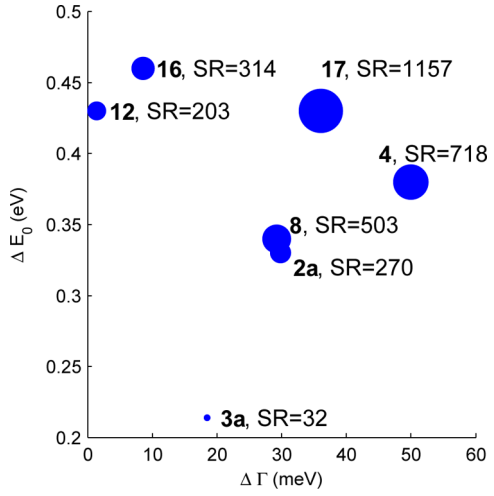

Figure 9. Magnitudes of the switching ratio (SR) as a function of the change of the closest MO (ΔE_0) and the coupling between the MO and the electrodes ($\Delta\Gamma$).

The behavior of the compounds studied here is different compared to the photoswitches studied previously by Kim et al. for which they obtained switching due to the change either in coupling to the electrodes[10] or in the relative position of the MO.[14] By the possibility to change both the coupling and the relative position of the MO, as in the case for compounds **4** and **17**, we can obtain a higher switching ratio compared to previous studied molecular photoswitches. At the same time the three criteria (i−iii) in the Introduction are fulfilled. Thus, they should represent good candidates of a new set of molecular conductance switches.

Stability and Realization. As pointed out by our criteria to a molecular switch, stability plays an important role, which is especially relevant to the suggested silane/silene based systems. It is known that silanes (OFF states) are persistent species at ambient conditions and could easily be inserted between two gold electrodes prior to switching applications. However, the silenes (ON states) are reactive, moisture sensitive, and have a high dimerization aptitude.[23] The situation can be significantly changed when the silanes are immobilized between the gold electrodes, and provided the concentration of silanes on the surface is low, the resulting spatial separation between the silenes when formed during switching will inhibit dimerization as a possible decomposition pathway. Moreover, the environment on the gold surface around the silane/silene switch can be covered by unreactive alkanethiols or alkanedithiols, e.g., as recently developed by us in a Au nanoparticle/nanoelectrode setup.[48] The incorporation of the silanes could be carried out by place-exchange.[49] The dimerization aptitude of the silenes

dx.doi.org/10.1021/jp400062y | J. Phys. Chem. C 2013, 117, 10909−10918

may also be reduced through a range of bulky substituents. The moisture sensitivity, on the other hand, is delicate, and the acylsilane/Brook-silene must likely operate under moisture-free conditions. However, reverse polarization, i.e., as observed for oxygen- or amino-substituted systems,[50] reduces moisture sensitivity of these silenes and might significantly increase the stability of the suggested molecular switches. For example, we found recently that 2-amino-2-siloxysilenes, which are transient silenes extensively influenced by reverse Si=C bond polarity ($Si^{\delta-}=C^{\delta+}$), are unreactive to alcohols.[51] It has also been observed that 1-silaallenes, i.e., Si=C double bonded compounds with an inherent $Si^{\delta-}=C^{\delta+}$ polarization influence, become resistant to water when they bear substituents with large steric bulk.[52]

CONCLUSIONS AND OUTLOOK

In conclusion, we have introduced a new class of synthetically realistic compounds that can perform as molecular conductance switches which could be triggered by light and/or thermal energy. Moreover, we were able to confirm that these switches fulfill the criteria for a useful reversible molecular switch, as given in the Introduction, i.e., a high ON/OFF conductance ratio, high enough barrier separating the two states, and a possibility to realize the switch in a solid state device. The reaction investigated is the [1,3]-silyl (germyl) shift from a low-conducting silane to a conducting silene, and the charge transport characteristics are investigated using DFT-NEGF calculations and a simple Landauer model. We started with a set of linear molecules and found by DFT-calculations that they can be switched photochemically in one way and switched back thermally. The single-molecule conductance showed good switching ratios at low bias; however, it was also found that large length variations when progressing along the reaction coordinate, especially at the TS, hamper their potential use as a solid state device.

To overcome this last issue we propose a cyclic central unit of the molecule reducing the flexibility while at the same time keeping the switching properties of the linear molecules. Calculations further show that we can tailor the reaction dynamics of the compounds, in terms of both reaction barrier (kinetics) and energy (thermodynamics) between the two states by changing the acceptor unit and/or the migration group. We find that the switching ratio is increased going from the linear molecules to the cyclic, and it is 200 or greater for all considered molecules at zero-bias voltage.

We have further analyzed the transport mechanism using the most conducting scattering state, the density of states in the junction, and a single-level Landauer model. We find that for the OFF states we have a MO localized in the central part of the molecule about 0.5 eV below E_F. We also see interference effects in some of the OFF states decreasing the transmission further. For the ON states, on the other hand, we have a delocalized π-electron system spanning the whole molecule and metal-induced gap states at E_F increasing the effective coupling to the electrodes. The most conducting MO is now (almost) resonant, enhancing the conductance significantly.

These results should be of great interest for the development of a solid state switch or memory device with a high ON/OFF conductance ratio and the possibility to be switched by two different stimuli (photochemically and thermally). With this study we propose a rearrangement and a class of compounds which are completely new to the field of molecular electronics, thus expanding the pool of compounds used in this research area.

ASSOCIATED CONTENT

Supporting Information

Full geometrical information and further computational details. This material is available free of charge via the Internet at http://pubs.acs.org.

AUTHOR INFORMATION

Corresponding Author

*E-mail: anton.grigoriev@physics.uu.se; henrik.ottosson@kemi.uu.se.

Notes

The authors declare no competing financial interest.

ACKNOWLEDGMENTS

We gratefully acknowledge Uppsala University through the U3MEC initiative (KoF07), the Higher Educational Commission (HEC) of Pakistan, the Swedish Research Council (Vetenskapsrådet), Carl Tryggers Stiftelse för Vetenskaplig Forskning, the Wenner-Gren Foundations, the Swedish Energy Agency, and Stiftelsen för Strategisk Forskning (SSF) for financial support. The Austrian Science Funds (FWF) is gratefully acknowledged for an Erwin Schrödinger Fellowship to A.O. [Project J 3193-N17]. The calculations were performed on resources provided by the Swedish National Infrastructure for Computing (SNIC) at C3SE, UPPMAX, and NSC.

REFERENCES

(1) Song, H.; Reed, M. A.; Lee, T. *Adv. Mater.* **2011**, *23*, 1583−1608.
(2) van der Molen, S. J.; Liljeroth, P. *J. Phys.: Condens. Matter* **2010**, *22*, 133001.
(3) Galperin, M.; Nitzan, A. *Phys. Chem. Chem. Phys.* **2012**, *14*, 9421−9438.
(4) Fuentes, N.; Martn-Lasanta, A.; Álvarez de Cienfuegos, L.; Ribagorda, M.; Parra, A.; Cuerva, J. M. *Nanoscale* **2011**, *3*, 4003.
(5) Liao, J.; Agustsson, J. S.; Wu, S.; Schönenberger, C.; Calame, M.; Leroux, Y.; Mayor, M.; Jeannin, O.; Ran, Y.-F.; Liu, S.-X.; et al. *Nano Lett.* **2010**, *10*, 759−764.
(6) Chen, F.; He, J.; Nuckolls, C.; Roberts, T.; Klare, J. E.; Lindsay, S. *Nano Lett.* **2005**, *5*, 503−506.
(7) Bogani, L.; Wernsdorfer, W. *Nat. Mater.* **2008**, *7*, 179−186.
(8) Benesch, C.; Rode, M. F.; Čížek, M.; Härtle, R.; Rubio-Pons, O.; Thoss, M.; Sobolewski, A. L. *J. Phys. Chem. C* **2009**, *113*, 10315−10318.
(9) van der Molen, S. J.; Liao, J.; Kudernac, T.; Agustsson, J. S.; Bernard, L.; Calame, M.; van Wees, B. J.; Feringa, B. L.; Schönenberger, C. *Nano Lett.* **2009**, *9*, 76−80.
(10) Kim, Y.; Hellmuth, T. J.; Sysoiev, D.; Pauly, F.; Pietsch, T.; Wolf, J.; Erbe, A.; Huhn, T.; Groth, U.; Steiner, U. E.; et al. *Nano Lett.* **2012**, *12*, 3736−3742.
(11) Choi, B.-Y.; Kahng, S.-J.; Kim, S.; Kim, H.; Kim, H.; Song, Y.; Ihm, J.; Kuk, Y. *Phys. Rev. Lett.* **2006**, *96*, 156106.
(12) Alemani, M.; Peters, M. V.; Hecht, S.; Rieder, K.-H.; Moresco, F.; Grill, L. *J. Am. Chem. Soc.* **2006**, *128*, 14446−14447.
(13) Smaali, K.; Lenfant, S.; Karpe, S.; Oçafrain, M.; Blanchard, P.; Deresmes, D.; Godey, S.; Rochefort, A.; Roncali, J.; Vuillaume, D. *ACS Nano* **2010**, *4*, 2411−2421.
(14) Kim, Y.; Garcia-Lekue, A.; Sysoiev, D.; Frederiksen, T.; Groth, U.; Scheer, E. *Phys. Rev. Lett.* **2012**, *109*, 226801.
(15) Lara-Avila, S.; Danilov, A. V.; Kubatkin, S. E.; Broman, S. L.; Parker, C. R.; Nielsen, M. B. *J. Phys. Chem. C* **2011**, *115*, 18372−18377.

(16) Brook, A. G.; Abdesaken, F.; Gutekunst, B.; Gutekunst, G.; Kallury, R. K. *J. Chem. Soc., Chem. Commun.* **1981**, 191−192.
(17) Brook, A. G.; Nyburg, S. C.; Abdesaken, F.; Gutekunst, B.; Gutekunst, G.; Krishna, R.; Kallury, M. R.; Poon, Y. C.; Chang, Y. M.; Winnie, W. N. *J. Am. Chem. Soc.* **1982**, *104*, 5667−5672.
(18) Eklöf, A. M.; Guliashvili, T.; Ottosson, H. *Organometallics* **2008**, *27*, 5203−5211.
(19) Morkin, T. L.; Leigh, W. J. *Acc. Chem. Res.* **2001**, *34*, 129−136.
(20) West, R. *Polyhedron* **2002**, *21*, 467−472.
(21) Gusel'nikov, L. E. *Coord. Chem. Rev.* **2003**, *244*, 149−240.
(22) Ottosson, H. H.; Steel, P. G. P. *Chem.−Eur. J.* **2006**, *12*, 1576−1585.
(23) Ottosson, H.; Eklöf, A. M. *Coord. Chem. Rev.* **2008**, *252*, 1287−1314.
(24) Bravo-Zhivotovskii, D. D.; Dobrovetsky, R. R.; Nemirovsky, D. D.; Molev, V. V.; Bendikov, M. M.; Molev, G. G.; Botoshansky, M. M.; Apeloig, Y. Y. *Angew. Chem., Int. Ed.* **2008**, *47*, 4343−4345.
(25) Chen, W.; Widawsky, J. R.; Vázquez, H.; Schneebeli, S. T.; Hybertsen, M. S.; Breslow, R.; Venkataraman, L. *J. Am. Chem. Soc.* **2011**, *133*, 17160−17163.
(26) Cheng, Z. L.; Skouta, R.; Vazquez, H.; Widawsky, J. R.; Schneebeli, S.; Chen, W.; Hybertsen, M. S.; Breslow, R.; Venkataraman, L. *Nat. Nanotechnol.* **2011**, *6*, 353−357.
(27) Frisch, M. J.; Trucks, G. W.; Schlegel, H. B.; Scuseria, G. E.; Robb, M. A.; Cheeseman, J. R.; Scalmani, G.; Barone, V.; Mennucci, B.; Petersson, G. A.; et al., *Gaussian 09*, Revision A.02; Gaussian Inc.: Wallingford CT, 2009.
(28) Becke, A. D. *J. Chem. Phys.* **1993**, *98*, 5648−5652.
(29) Stephens, P. J.; Devlin, F. J.; Chabalowski, C. F.; Frisch, M. J. *J. Phys. Chem.* **1994**, *98*, 11623−11627.
(30) Hariharan, P. C.; Pople, J. A. *Theor. Chim. Acta* **1973**, *28*, 213−222.
(31) Eklöf, A. M. Low coordinated Silicon and Hypercoordinated Carbon: Structure and Stability of Silicon Analogs of Alkenes and Carbon Analogs of Silicates. Ph.D. thesis, Uppsala University, Department of Biochemistry and Organic Chemistry, 2008.
(32) Zhao, Y.; Truhlar, D. G. *Acc. Chem. Res.* **2008**, *41*, 157−167.
(33) Zhao, Y.; Truhlar, D. G. *Theor. Chem. Acc.* **2007**, *120*, 215−241.
(34) Krishnan, R.; Binkley, J. S.; Seeger, R.; Pople, J. A. *J. Chem. Phys.* **1980**, *72*, 650−654.
(35) Brandbyge, M.; Mozos, J.-L.; Ordejon, P.; Taylor, J.; Stokbro, K. *Phys. Rev. B* **2002**, *65*, 165401.
(36) Soler, J. M.; Artacho, E.; Gale, J. D.; Garcia, A.; Junquera, J.; Ordejon, P.; Sánchez-Portal, D. *J. Phys.: Condens. Matter* **2002**, *14*, 2745−2779.
(37) Artacho, E.; Anglada, E.; Diéguez, O.; Gale, J. D.; Garca, A.; Junquera, J.; Martin, R. M.; Ordejon, P.; Pruneda, J. M.; Sanchez-Portal, D.; et al. *J. Phys.: Condens. Matter* **2008**, *20*, 064208.
(38) Troullier, N.; Martins, J. L. *Phys. Rev. B* **1991**, *43*, 1993.
(39) Perdew, J. P.; Wang, Y. *Phys. Rev. B* **1992**, *45*, 13244−13249.
(40) Aviram, A.; Ratner, M. A. *Chem. Phys. Lett.* **1974**, *29*, 277−283.
(41) Schiessling, J.; Grigoriev, A.; Stener, M.; Kjeldgaard, L.; Balasubramanian, T.; Decleva, P.; Ahuja, R.; Nordgren, J.; Brühwiler, P. A. *J. Phys. Chem. C* **2010**, *114*, 18686−18692.
(42) Paulsson, M.; Brandbyge, M. *Phys. Rev. B* **2007**, *76*, 115117.
(43) Solomon, G. C.; Herrmann, C.; Hansen, T.; Mujica, V.; Ratner, M. A. *Nat. Chem.* **2010**, *2*, 223−228.
(44) Okabayashi, N.; Paulsson, M.; Ueba, H.; Konda, Y.; Komeda, T. *Phys. Rev. Lett.* **2010**, *104*, 077801.
(45) Odell, A.; Delin, A.; Johansson, B.; Rungger, I.; Sanvito, S. *ACS Nano* **2010**, *4*, 2635−2642.
(46) Büttiker, M.; Imry, Y.; Landauer, R.; Pinhas, S. *Phys. Rev. B* **1985**, *31*, 6207−6215.
(47) Di Ventra, M. *Electrical Transport in Nanoscale Systems*; Cambridge University Press: Cambridge, 2008.
(48) Wallner, A.; Jafri, S. H. M.; Blom, T.; Gogoll, A.; Leifer, K.; Baumgartner, J.; Ottosson, H. *Langmuir* **2011**, *27*, 9057−9067.
(49) Liao, J.; Bernard, L.; Langer, M.; Schönenberger, C.; Calame, M. *Adv. Mater.* **2006**, *18*, 2444−2447.
(50) Ottosson, H. *Chem.−Eur. J.* **2003**, *9*, 4144−4155.
(51) Guliashvili, T.; Tibbelin, J.; Ryu, J.; Ottosson, H. *Dalton Trans.* **2010**, *39*, 9379−9385.
(52) Miracle, G. E.; Ball, J. L.; Powell, D. R.; West, R. *J. Am. Chem. Soc.* **1993**, *115*, 11598−11599.